DIAGNOSTICS

A dye-assisted paper-based point-of-care assay for fast and reliable blood grouping

Hong Zhang,[1,2]* Xiaopei Qiu,[1,2]* Yurui Zou,[1,2] Yanyao Ye,[3] Chao Qi,[3] Lingyun Zou,[4] Xiang Yang,[5] Ke Yang,[5] Yuanfeng Zhu,[6] Yongjun Yang,[6] Yang Zhou,[5] Yang Luo[1,2]†

Fast and simultaneous forward and reverse blood grouping has long remained elusive. Forward blood grouping detects antigens on red blood cells, whereas reverse grouping identifies specific antibodies present in plasma. We developed a paper-based assay using immobilized antibodies and bromocresol green dye for rapid and reliable blood grouping, where dye-assisted color changes corresponding to distinct blood components provide a visual readout. ABO antigens and five major Rhesus antigens could be detected within 30 s, and simultaneous forward and reverse ABO blood grouping using small volumes (100 μl) of whole blood was achieved within 2 min through on-chip plasma separation without centrifugation. A machine-learning method was developed to classify the spectral plots corresponding to dye-based color changes, which enabled reproducible automatic grouping. Using optimized operating parameters, the dye-assisted paper assay exhibited comparable accuracy and reproducibility to the classical gel-card assays in grouping 3550 human blood samples. When translated to the assembly line and low-cost manufacturing, the proposed approach may be developed into a cost-effective and robust universal blood-grouping platform.

INTRODUCTION

Rapid and accurate blood grouping plays a critical role in multiple scientific disciplines, particularly in the biological and medical sciences (*1*, *2*). Among the 35 officially recognized blood group systems, the ABO and Rhesus (Rh) systems receive the most attention because of the high mortality originating from mismatched ABO/Rh blood transfusion reactions (*3*–*5*). Conventional approaches to blood grouping, which are dominated by microplate-based (*6*) and gel column–based (*7*) assays, are encumbered by long turnaround times, labor-intensive operation, and technical training requirements, imposing financial burden on the health care system (*8*). Therefore, developing a simple and economical strategy for fast blood grouping would facilitate the accessibility and use of this tool in emergencies and resource-limited areas (*9*, *10*).

Paper-based assays, which are rapid, convenient, and inexpensive, hold promise for point-of-care (POC) blood grouping with a readout visible to the naked eye (*11*, *12*). However, the previously reported approaches depend on either the recognition of red blood cell (RBC) clots (*13*, *14*) or the distance gap of wicking between RBCs and plasma after separation (*15*, *16*), which prevents accurate discrimination between nonblood solutions that resemble type O blood because specific RBC membrane antigens are absent in both types of samples. Although a reverse ABO grouping strategy can somewhat decrease these risks by identifying serum agglutinins, the requirement for centrifugation-based plasma separation before reverse grouping is not always practical (*17*). To date, no reliable methodologies that integrate forward and reverse (F&R) tests into one assay have been proposed, although there have been a few attempts (*18*, *19*).

Here, an easy-to-interpret dye-assisted paper-based (DAP) assay for blood grouping is proposed, which integrates the F&R tests into a single POC chip using a visual readout strategy. Forward grouping identifies specific antigens on RBCs, whereas reverse grouping detects antibodies in plasma on the basis of RBC agglutination. The newly established DAP strategy is founded on the ability of human serum albumin (HSA) to react with the yellow monoanionic dye bromocresol green (BCG) to produce a teal BCG-HSA complex in an acidic environment, whereas whole blood produces a brown complex after reacting with BCG, which is easily distinguished with the naked eye. We optimized various operating characteristics to fabricate a simultaneous F&R ABO assay and an ABO forward assay with a combined ABO/Rh (A/B/D/C/c/E/e antigens) assay, both of which test uncentrifuged blood. A total of 3550 clinical human blood samples were tested to validate the robustness of the proposed DAP blood-grouping platform.

RESULTS

The dye-based readout mechanism for blood grouping

The accurate and reliable recognition of blood agglutination events is a prerequisite for developing a reliable blood-grouping assay, which is conventionally performed by observing blood aggregation in the presence of specific antigens or hemagglutinins. In principle, only serum can migrate along the porous chromatographic paper used in a paper-based assay after the RBCs are aggregated, whereas both serum and RBCs can migrate freely along the substrate if the RBCs remain nonaggregated. Thus, the ability to accurately distinguish chromatographic products is a promising biosensing mechanism for rapid blood grouping.

HSA can act as a sensitive indicator of human plasma because it comprises about 60% of the total serum proteins (*20*). Among HSA-determining assays, the BCG-based dye-binding method is economical and convenient. HSA reacted with the yellow monoanionic dye BCG (pH 4.2) to generate a teal BCG-HSA complex (λ_{max} = 630 nm) in the presence of a nonionic surfactant (Brij-35) (Fig. 1, A and B). In contrast, whole blood induced the formation of a brown complex under the

[1]Center for Nanomedicine, Southwest Hospital, Third Military Medical University, Chongqing, China. [2]Department of Clinical and Military Laboratory Medicine, School of Medical Laboratory Science, Southwest Hospital, Third Military Medical University, Chongqing, China. [3]Department of Blood Transfusion Medicine, Southwest Hospital, Third Military Medical University, Chongqing, China. [4]College of Basic Medical Sciences, Third Military Medical University, Chongqing, China. [5]Department of Laboratory Medicine, Southwest Hospital, Third Military Medical University, Chongqing, China. [6]Medical Research Center, Southwest Hospital, Third Military Medical University, Chongqing, China.
*These authors contributed equally to this work.
†Corresponding author. Email: luoyang@tmmu.edu.cn

same conditions (Fig. 1B), likely due to the color overlap of BCG-RBC and BCG-HSA, which was validated by the coexistence of the characteristic absorbance peaks of the BCG-plasma and BCG–whole blood complexes (Fig. 1C). The two complexes shared an identical characteristic absorbance peak at 630 nm, whereas the BCG–whole blood complex displayed three other absorbance peaks at 530, 540, and 570 nm, suggesting that a spectral analysis can be used to eliminate subjective color errors to ensure analytical accuracy and to the benefit of color-blind and color-weak assay users. Protein-free solutions such as phosphate-buffered saline (PBS) (no color change) and red ink–mimicking blood tinctures (dark red) do not react with BCG, making it easy to distinguish them from blood (Fig. 1B). Thus, BCG can act as a bifunctional reagent that provides a detection reagent for the differentiation of plasma and whole blood, as well as a built-in quality control to exclude protein-free solutions.

DAP test for fast and flexible blood grouping

Using the above BCG biosensing mechanism, we developed a series of blood-grouping formats that meet various clinical requirements: a fast ABO forward and ABD (ABO and Rh D) test for emergency use, an ABO F&R format and an ABO/Rh format (A/B/D/C/c/E/e) for routine clinical tests, and a rare group format for specialized applications. The proposed ABO forward format (Fig. 2A and fig. S1A) can yield visual results within 30 s after successively loading 15 μl of whole blood and 30 μl of eluent. If specific RBC antigens are present in the blood, the corresponding coated immunoglobulin M (IgM) antibodies will capture the RBCs and only the plasma will migrate to the detection zone (BCG-coated) to induce a teal color readout, whereas a brown color will appear if specific RBC antigens are absent.

The successful construction of an ABO forward assay spurred the integration of the ABO F&R blood groups into a single chip. As illustrated in Fig. 2B, the proposed F&R assay has two independent array strips, the F strip and the R strip for F&R blood grouping, respectively. Armed with the capability to separate plasma from whole blood using a blood separation membrane, the proposed assay achieved simultaneous F&R grouping on one chip (Fig. 2B), representing a considerable advance compared with conventional assays that require centrifugation to separate the plasma. After the plasma is separated by the blood separation membrane, the loaded RBC reagent aggregates and the remaining plasma migrates to the BCG detection zone after elution to form the BCG-HSA complex (teal) in the presence of specific plasma agglutinins. Otherwise, both the RBC reagent and the plasma migrate to the BCG zone to form the BCG–whole blood complex (brown). This mechanism allowed the rapid F&R grouping assay to produce a visual colorimetric readout within 2 min. Notably, 90 s of the 2-min time is attributed to the additional plasma filtering and RBC reagent loading steps required for this assay.

A similar principle was used to fabricate an ABD format that is capable of simultaneously detecting ABO and Rh D within 30 s by loading 30 μl of whole blood and 60 μl of eluent (fig. S1B). Additionally, an integrated ABO/Rh format was mounted on one POC disc for the simultaneous grouping of both ABO and Rh groups within 30 s. In this assay, only 80 μl (10 μl for each channel) of whole blood was used in the reactions with the diverse immobilized antibodies (A/B/D/C/c/E/e) in different channels of the disc (Fig. 2C). The rare group format permits rare blood typing by immobilizing the corresponding antibodies [MNS (M, N, S, s), P (P1), Kell (K, k), Kidd (Jk^a, Jk^b), Lewis (Le^a, Le^b), and Duffy (Fy^a, Fy^b)] on a POC disc similar to the assay shown in Fig. 2C and requires an observation time of 2 min because several antigens have longer agglutination times.

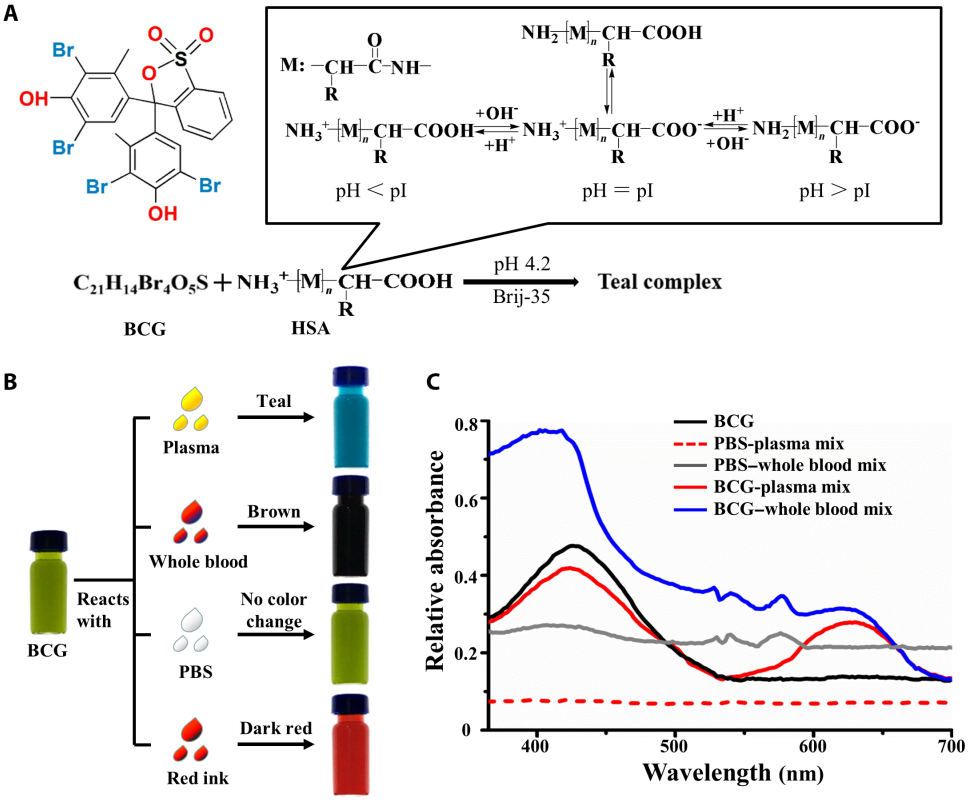

Fig. 1. Mechanism of the dye-based visual readout for fast blood grouping. (**A**) Chemical structures of BCG ($C_{21}H_{14}Br_4O_5$) and HSA and the principle of the BCG-HSA reaction. (**B**) Color changes observed when BCG reacted with plasma (teal), whole blood (brown), PBS (no color change), and red ink (dark red). (**C**) Relative absorbance values for BCG (black line), PBS-plasma (red dashed line), PBS–whole blood (gray line), the BCG-plasma complex (red line), and the BCG–whole blood complex (blue line).

Operating characteristics

Substrate selection and optimization of the reagent concentrations.

An appropriate paper substrate is essential to fabricate a reliable paper-based strip. Although it is widely used in lateral flow immunochromatography assays, a conventional nitrocellulose (NC) membrane was not suitable in our setting because blood samples migrate slower on NC membranes than on other substrates (fig. S2A). In contrast, fiberglass paper with the largest pore size displayed the fastest blood migration rate during 120-s continuous observations; thus, fiberglass paper was adopted to fabricate the sampling and the hydrophobic chromatography pad (fig. S2A). A cotton linter paper with a condensed fiber structure was used as the pad

for antibody and BCG immobilization, and the protein-binding capacity was validated by both visual observations and microscopy (fig. S2, B to D).

A Jieyi glass fiber II (GF2) microglass fiber membrane had a much higher plasma-separating efficiency as the plasma separation membrane in the reverse strip than several other plasma separation membranes, such as Vivid GR, Cobetter, and Whatman MF1, mainly due to their different flow directions and paper microstructures (fig. S2, E and F, and table S1). The proposed F&R assay composed of these paper substrates exhibited fast blood grouping, without the need for a separate centrifugation procedure.

Optimal antigen and antibody concentrations were established to improve the analytical efficiency of the DAP assays. A 20% RBC dilution was the minimum concentration that produced easily detectable results in the reverse typing because lower RBC concentrations failed to induce an obvious color change (fig. S3A). A titer-dependent optical density profile was established by introducing a series of dilutions of seven antibodies (anti-A/B/D/C/c/E/e). The results suggested that a 1:32 dilution was the optimal concentration for the anti-A, anti-B, and anti-E antibodies, a 1:64 dilution was optimal for the anti-D antibody (fig. S3B), and a 1:16 dilution was sufficient for the other antibodies (table S2).

Notably, the long-term stability of the immobilized antibodies was ensured by adding StabilGuard Immunoassay Stabilizer to the IgM solutions, and the results obtained after 6 months were identical to the results obtained with fresh blood samples (fig. S4A). We further determined the influence of the reaction time on the results by recording the color intensity of the BCG zone at 30-s intervals after introducing HSA for a total of 10 min (fig. S4B). A time-dependent increase in the color intensity of the BCG-HSA complex was observed, reaching a peak at 30 s. Subsequently, no apparent change in the color intensity was observed at 10 min (fig. S4C), although slow binding reactions between BCG and other proteins, such as α- and β-globulins, may occur.

Spectral characterization and recognition of potential interference.

Fluorescence was examined to visualize the formation of agglutinated RBCs and to validate the authenticity of this agglutination-based

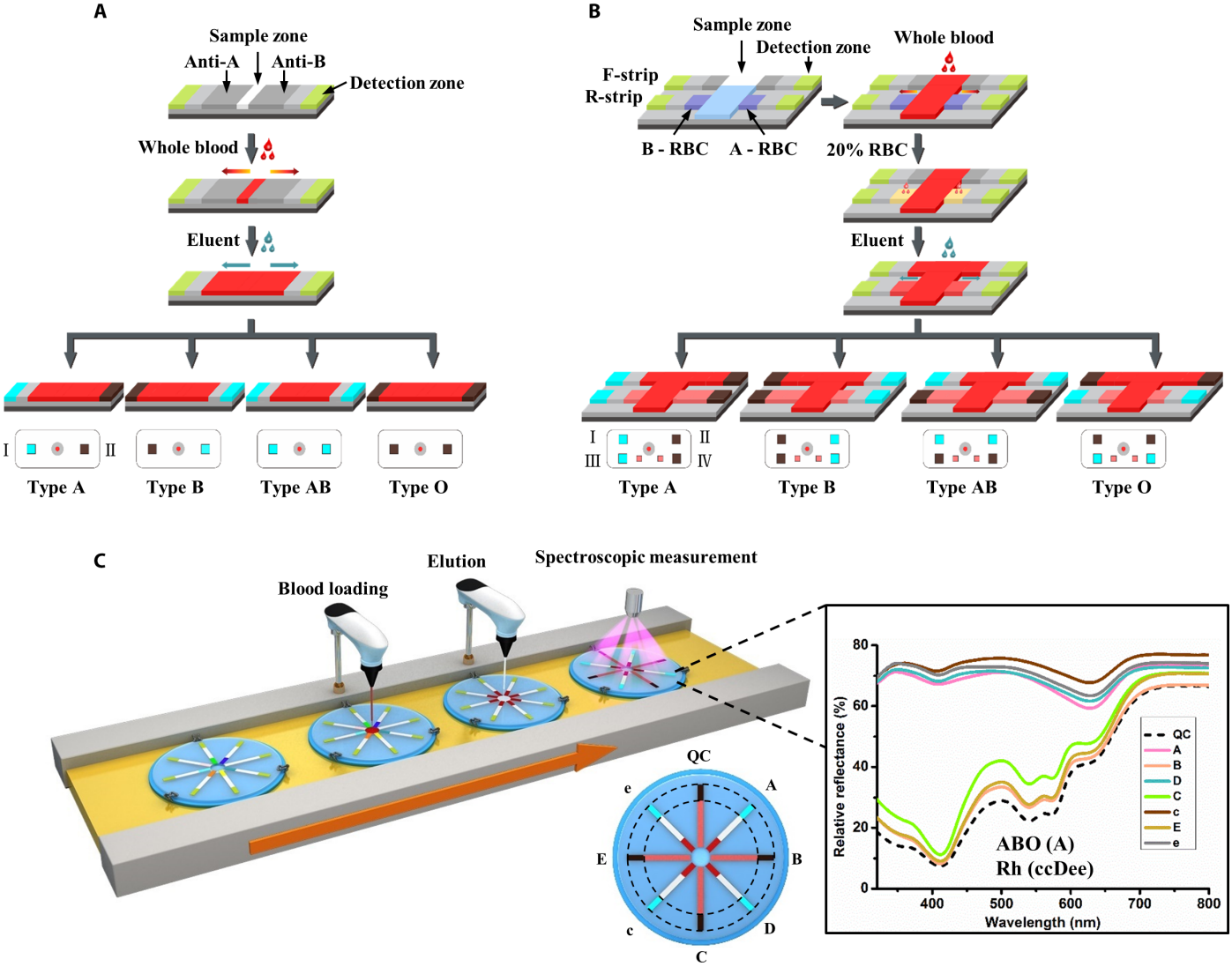

Fig. 2. Schematic of the fast blood-grouping devices. Designs, testing procedures, and results of our (**A**) ABO forward strip, (**B**) F&R assay, and (**C**) ABO and Rh group multiplex antigen assays. I and II represent the forward blood-grouping observation windows; III and IV represent the reverse blood-grouping observation windows. The observation zone is located between the two dotted lines as shown in the platforms of the ABO and Rh group assays (C). A strip without antibody (BCG only) was used for quality control (QC).

blood-grouping test. Confocal imaging revealed the agglutinated RBCs on the antibody-immobilized substrate (Fig. 3A). If the RBCs were not agglutinated (Fig. 3B), both red fluorescein (HSA) and green fluorescein (RBC) were observed (Fig. 3C); otherwise, only red fluorescein was observed (Fig. 3D). This finding was also verified using a spectrophotometer, which revealed distinguishable waveforms of the reflectance curves for the BCG-HSA complex, BCG–whole blood complex, and other nonblood samples (Fig. 3E). Notably, the BCG-plasma complex displayed characteristic peaks at both 410 and 630 nm, whereas the BCG–whole blood complex showed additional peaks at 410, 540, and 570 nm. As shown in Fig. 3E, both the nonblood samples (PBS and red ink) and the void strip (mimicking inactivated BCG) could be effectively distinguished from blood samples using the characteristic peaks, suggesting an improvement over the existing paper-based blood-grouping methodologies that are incapable of identifying nonblood samples.

An unexpected color change may occur in aqueous solutions with pH values that are higher than the BCG dissociation constant (pKa = 4.8), in which the monoanionic BCG (yellow) would convert to the dianionic form (teal) through further deprotonation (*21*). The eluent was sufficiently buffered to maintain an acidic environment (the optimal pH 4.20 for HSA detection) and eliminate this interference, even when it was mixed with acidic (pH 3.60) or basic (pH 11.20) blood samples (*22*). A teal color was observed for both acidic and basic blood in the presence of a nonionic surfactant, suggesting that the influence of blood pH on the grouping results of traditional blood samples (pH of about 7.40) is negligible (fig. S5A). Additionally, blood samples from uremic patients with electrolyte disturbance were tested by incubating the samples with the BCG solution to observe the effects of ionic strength on color definition and intensity (table S3), and no significant difference in the color change was observed ($P = 0.84$, $n = 10$) (fig. S5B).

Because hematocrit (HCT) values vary widely in certain clinical populations, such as pregnant women (30 to 38%) and newborns (48 to 68%) (*23*), we investigated the influence of different HCT values on antigen-antibody reaction and plasma separation rates (fig. S6, A to D). In the ABO forward test, a sufficient amount of antibody was coated to compensate for high HCT (76.7%) and to avoid any postzone phenomenon (absence of precipitation with excess antigen). In the reverse strip, the results showed that a 1.96-cm^2 GF2 plasma separation membrane was sufficient to capture 100% of the RBCs from 100 μl of whole blood with 76.7% (about 23.3 μl of plasma) (fig. S6C) or 20.8% (about 79.2 μl of plasma) (fig. S6B) of HCT, and all 50 blood samples were correctly grouped in the F&R tests, suggesting that the interference from fluctuating HCT values is negligible. No significant differences were observed in the reflectance curves for HSA levels ranging from 13.7 to 52.6 g/liter ($P = 0.79$ for zone I, $P = 0.94$ for zone II, $P = 0.89$ for zone III, and $P = 0.85$ for zone IV), indicating that the effect of endogenous HSA on the grouping results was negligible, regardless of the concentration-dependent color intensity of the BCG-HSA complex in solution (fig. S6, E to H).

Additionally, the maximal storage periods for whole blood were explored by adding several prevalent anticoagulants including EDTA, sodium citrate, and heparin. Blood that was treated with the different anticoagulants yielded identical results to fresh blood if the storage time was less than 8 days (Fig. 4A and fig. S7), and only a slight hemolysis occurred [free hemoglobin (FHB) ≤ 74.85 mg/liter] (Fig. 4B). As expected, extended storage (>12 days), wherein substantial hemolysis occurred (FHB > 174.67 mg/liter), increased the risks of weaker agglutination and false type O results (Fig. 4B). Notably, the relative reflectance of the BCG-plasma complex at 410 nm was much higher than the BCG-blood complex in storage for 8 days or less, whereas the relative reflectance curve of the BCG-plasma complex switched to the curve of the BCG-blood complex after storage for more than 8 days (Fig. 4C). This change primarily occurred because the RBCs that would have agglutinated before a substantial number of RBCs ruptured instead

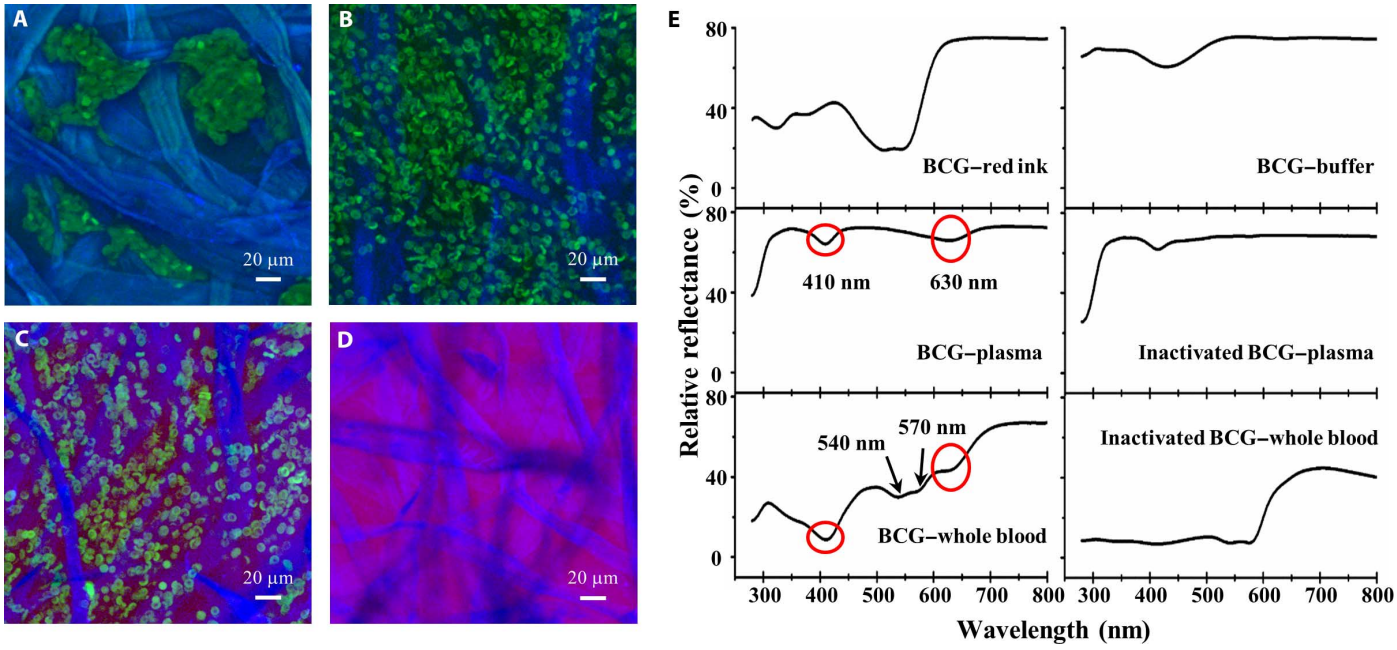

Fig. 3. Characterization of the results of the DAP blood grouping using fluorescein and spectrophotometry. Confocal images of (**A**) agglutinated RBCs, (**B**) nonagglutinated RBCs, (**C**) nonagglutinated RBC-HSA, and (**D**) HSA within the paper. RBCs, green; HSA, red; cotton linter paper, blue. (**E**) Divergent waveforms of the reflectance curves for BCG–red ink, BCG-plasma, BCG–whole blood, BCG-PBS, plasma, and whole blood. Circle regions denote the shared characteristic peaks at 410 and 630 nm for both BCG-plasma and BCG–whole blood samples. Arrows are the newly appeared peaks for BCG–whole blood mix when compared with BCG-plasma mix.

reacted with BCG, causing the blood to be mistakenly recognized as type O. Because solutions with a lower concentration tend to exhibit a higher reflectance but an identical curve, the difference between detection zones IV (BCG–20% RBC and plasma) and II (BCG–whole blood) in Fig. 4A likely resulted from the different RBC concentrations.

The effects of ambient temperature, humidity, and light on the dye-assisted color change visual readout were also investigated. We did not observe a noticeable difference in the BCG-HSA reaction at temperatures of 5°, 25°, 45°, and 65°C and relative humidities (RHs) of 30, 60, and 90% (fig. S8, A and B). Light strengths of 1500, 3000, 4500, and 6000 lux affected the visual results, but no apparent changes in the characteristic absorbance peak at 630 nm were measured (fig. S8C). Because the visual color change is affected by the ambient light intensity and individual mood or eye conditions, we recommend the use of automatic measurements with reflective spectroscopy to avoid these inconsistencies.

Evaluation of the methodology using clinical samples.

A machine-learning strategy was used to automatically classify various blood types and to adapt the method to an automated testing platform. Classification performance was tested using a 10-fold cross-validation during the examination of a reflectance data set that accurately tested all entries, including 600 blood samples and 15 invalid samples (5 BCG–red ink, 5 BCG-PBS, and 5 BCG only). The 15 invalid samples were recognized with 100% accuracy (fig. S9). The proposed support vector machine (SVM) system demonstrated an accuracy of 99.9%, a sensitivity of 99.9%, and a specificity of 100% for the ABO F&R blood groups. The feasibility of the proposed DAP blood grouping was also validated by an area under the curve (AUC) of 0.999 (fig. S10) and a Matthews correlation coefficient (MCC) of 0.999.

We also compared the results of our large-scale DAP assays of blood samples with the results from a gel-card assay. An accuracy of 100% was obtained for 800 blood samples during the ABO forward assay (Fig. 5A, fig. S11, A and B, and table S4) and for 50 samples during the ABD forward assay (fig. S11, C and D). For the 1400 blood samples tested using the F&R assay, including 38 weak-agglutination samples from newborns and leukemia patients, the F&R assay was accurate (99.93%), and only one A_1 sample from a leukemia patient was incorrectly identified (Fig. 5B, fig. S12, and table S5).

For the ABO/Rh assay, the analysis of an additional 1200 blood samples revealed 99.92% accuracy for both the ABO and the Rh blood groups (Fig. 5C, fig. S13, A and B, and table S6). Among these samples, 15 clinical subtypes (4 A_2, 1 A_3, and 10 weak Rh D) were detected (fig. S13C)—4 A_2 and all the Rh D samples were correctly grouped, whereas an A_3 sample was incorrectly recognized as type O, likely due to the inefficiency of the immobilized anti-A IgM antibody in capturing A_3. We tested 100 blood samples for rare grouping [MNS (M, N, S, s), P (P1), Kell (K, k), Kidd (Jk^a, Jk^b), Lewis (Le^a, Le^b), and Duffy (Fy^a,

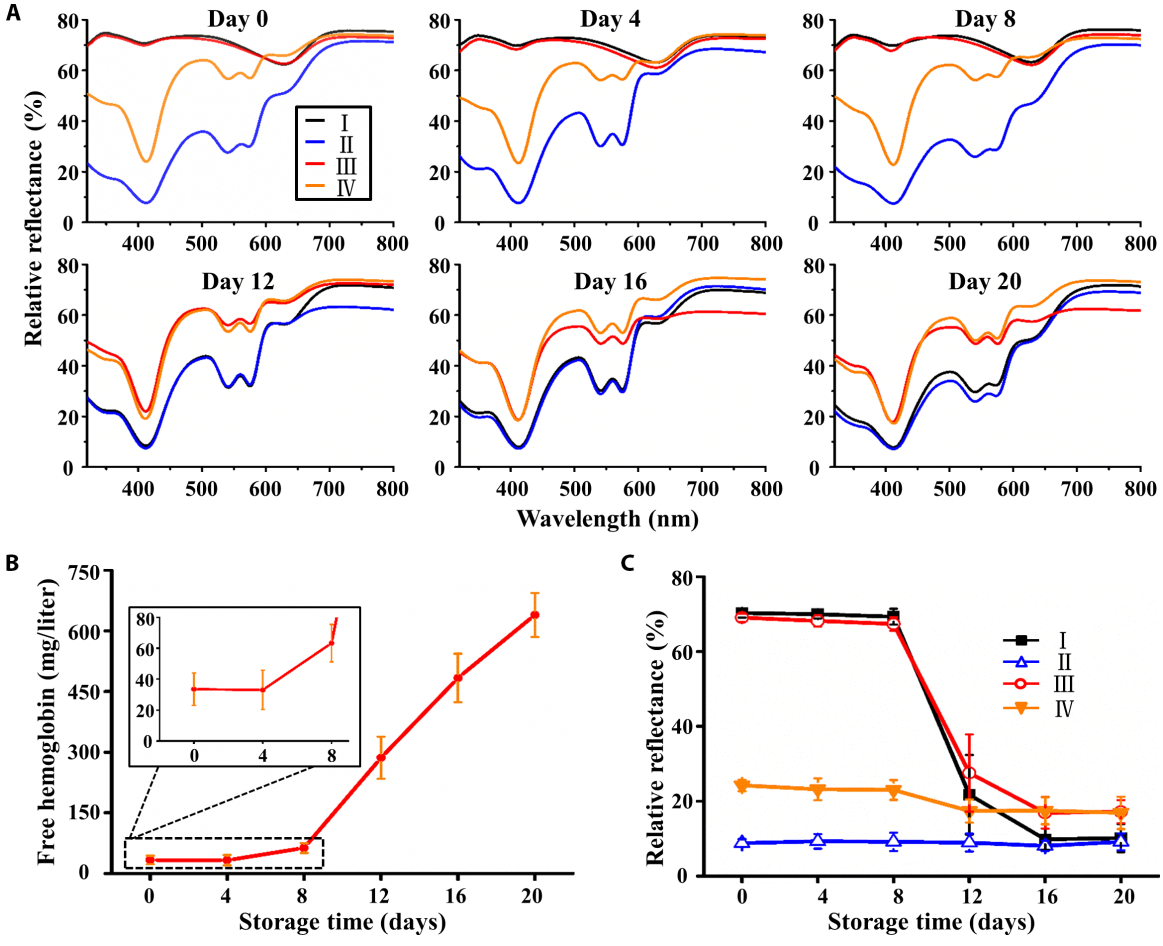

Fig. 4. Evaluating the feasibility of detecting stored samples (type A). (**A**) Relative reflectance curves of blood samples stored for 0 to 20 days before testing using the F&R assay. I and II represent the observation windows for the forward blood grouping; III and IV represent the observation windows for the reverse blood grouping. (**B**) FHB concentration in samples stored for 0 to 20 days before testing. (**C**) Relative reflectance of the detection zones (I, II, III, and IV) at 410 nm for samples stored for 0 to 20 days before testing.

Fy^b)], all of which were successfully detected using both methods (Fig. 5D, fig. S14, and table S7). Fifty samples were detected in triplicate within 1 day and assayed consecutively for an additional 8 days to confirm the reproducibility of the proposed assays (fig. S15). Inconsistent results were not observed, indicating that our proposed assay has excellent reproducibility.

DISCUSSION

The accurate identification of human blood systems is essential to avoid incompatible transfusions (*24*). We designed and developed a DAP test for rapid blood grouping using a newly developed dye-based readout strategy to conquer long-standing problems with conventional methodologies, such as long turnaround times (*25*), labor-intensive operation (*26*), and technical training requirements (*27*). On the basis of color change resulting from the reaction of BCG with albumin, our blood-grouping readout strategy has the following exclusive advantages: (i) simultaneous ABO F&R grouping within 2 min and (ii) rapid testing of ABO forward/ABD grouping and combined ABO/Rh grouping within 30 s.

Conventional blood-grouping methods, including the gel-card assay, have moderate sensitivity and accuracy but are time-consuming (10 to 20 min) (*28*, *29*). New technologies, such as paper-based (*30*, *31*) (30 s to 3 min) and thread-based (*16*, *32*) platforms (<1 min) and microfluidic chips (*33*–*35*) (3 to 5 min), permit direct readout in clinical assays, without the requirement for complicated indoor equipment (*36*); however, a sophisticated readout algorithm (*37*) or experienced personnel are still required, and a separate centrifugation step to isolate plasma is essential for reverse grouping. In our proof-of-concept experiment, we used the rapid reaction between albumin and BCG and spectral detection based on agglutination to substantially reduce the analytical time without compromising specificity and sensitivity. Both ABO (A/B) and Rh (D/C/c/E/e) blood group antigens were differentiated within 30 s, whereas ABO F&R blood grouping required 2 min.

Considerable efforts have been devoted to develop an assay capable of simultaneous F&R ABO grouping by loading the sample once, but no such assays have yet been proposed. Spindler *et al.* (*18*) described an attempt at F&R grouping based on the formation of an RBC monolayer on a microplate, but their method still required centrifugation before reverse grouping, as well as multiple sample loading cycles; thus, the method did not meet the definition of simultaneous. Noiphung *et al.* (*38*) proposed a paper-based analytical device for blood typing that allows the simultaneous determination of ABO and Rh blood groups on the same device. However, the HCT in the sample can affect the accuracy of the results, and appropriate dilution is required before grouping. In contrast, our BCG-based assay overcame the requirement for centrifugation and the influence of HCT levels observed in previous F&R ABO grouping methods, which is attributed to the introduction of a plasma separation pad that enabled rapid plasma separation for the subsequent reverse tests and a new readout mechanism.

Additionally, a machine-learning method has been used to ensure the accuracy of blood grouping, by which the influence of subjective judgment that is susceptible to ambient factors and diverse color discernibility could be eliminated. We have noticed that the reflectivity at a single wavelength poorly reflected the overall trend of the whole reflective spectrum. Experimentally, the measured reflectivities at 410 nm for samples with high HCT values were significantly lower than those with low HCT values, whereas the results from a machine-learning method gave identical results among these samples with high, low, and normal HCT values, indicating that a machine-learning method can provide higher accuracy. Moreover, a machine-learning method can expand the applicability of the proposed DAP assay by providing the potential to develop into a fully automatic platform for massive grouping in routine clinical practice.

Notably, false-negative results may appear in the serological grouping of several rare blood group systems, mainly due to the influences of variant or less antigenic

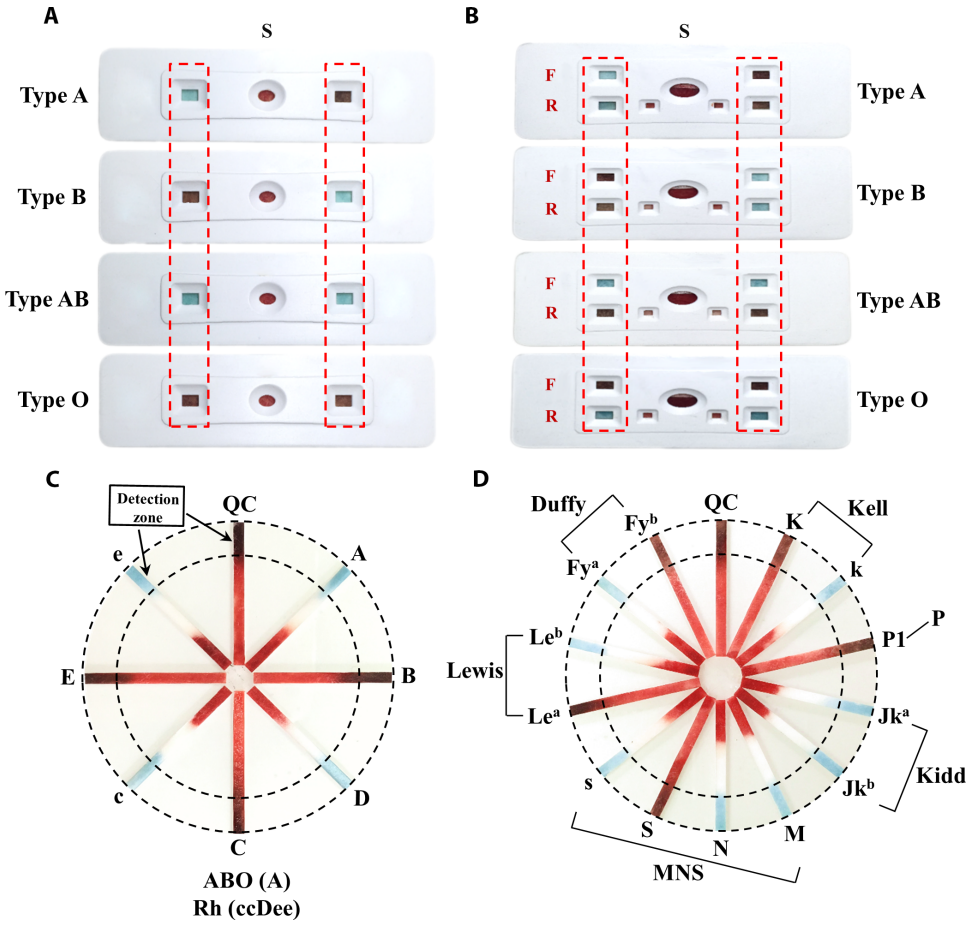

Fig. 5. Results of the visual readout for fast blood grouping. Images of (**A**) forward strip and (**B**) F&R assays showing ABO grouping for A, B, AB, and O as indicated by the presence of teal color in the observation zone (red dashed box). Images of multiplexed assays testing (**C**) ABO/Rh and (**D**) rare blood systems. The sample in (C) is ABO (A)/Rh (ccDee); the samples in (D) show Kell (K^-k^+), P (P2), Kidd ($Jk^{a+}Jk^{b+}$), MNS (MNss), Lewis ($Le^{a-}Le^{b+}$), and Duffy ($Fy^{a+}Fy^{b-}$).

antigens, insufficient reaction times, or ambient temperature. For instance, the Lewis (Le) group system is particularly affected by the external conditions because its RBC antigens are adsorbed. Grouping relies on the glycolipid that carries the Le structure on the cytomembrane because the glycolipid cannot complex with antigens with a type I skeleton. An increased prevalence of the Le (a-b-) phenotype resulting from a reduction in the adsorbed antigens has been reported in conditions such as alcoholic cirrhosis, alcoholic pancreatitis, and normal pregnancy (*39*, *40*). Regarding the Duffy group, false-negative results are frequently reported for the Fy^a/Fy^x antigen (the Fy^x antigen produced by the Fy^x allele is generally regarded as a weak Fy^b antigen) because of the weakened reaction between the anti-Fy^b antibody and the Fy^a/Fy^x antigen (*41*). Although the results of the proposed DAP test and gel-card method are comparable, caution should be used under these clinical conditions when rare group systems are tested. We have taken measures to minimize these influences by adopting high-titer antibodies and dextran to maintain the stabilities of the antibodies. Additionally, the observation time was extended to 15 min for these negative results during rare group typing (Le, P, and Duffy), and no visible RBC agglutination was observed, validating the reliability of the DAP assay. No positive results were observed for the P1 phenotype during our clinical detection, although it is present in 35% of the overall Chinese population. We reasoned that the inconsistency might be attributed to biased sampling because 12 of the 100 samples were obtained from 3- to 6-year-old children whose P1 antigen is not completely formed.

The proposed DAP assay is a promising solution because it combines the advantages of flexibility, economy, and synchronization of ABO F&R grouping. Nevertheless, several limitations exist in the proposed assay. First, we must improve the ability to determine certain existing weak agglutination types (A_x, B_x, and A_3), which may be achieved by engineering enhanced antibodies. Second, the proposed systems cannot sufficiently distinguish blood samples from other protein-containing solutions because BCG can react with any protein to produce a teal complex. Third, factors derived from various pathological conditions and medications that may potentially interfere in the visual readout of the assay still need further evaluation. Finally, the proposed DAP test, like any serological-based blood-grouping assay, is susceptible to the expression levels of blood group antigens and the integrity of the RBC membrane.

A fast, reliable, and versatile blood-grouping assay with a dye-based readout mechanism is proposed for the simultaneous identification of both ABO and Rh blood group systems within 30 s or simultaneous ABO F&R grouping or rare blood typing within 2 min. This assay not only provides a new strategy for blood grouping but can also be used in time- and resource-limited situations, such as war zones, in remote areas, and during emergencies. Characterized by an intensified and streamlined workflow capability, the proposed blood-grouping assay may be further developed into highly compact and fully automatic platforms that are highly efficient and economical, making large-scale manufacturing possible (*42*).

MATERIALS AND METHODS

Study design

This study was designed to develop a dye and paper-based blood-grouping assay for efficient and reliable simultaneous F&R blood typing. The assay is based on BCG, which immediately changes color in the presence of protein. The effects of environmental factors such as temperature, humidity, and light intensity on BCG-plasma reactions were assessed. The absorbance of BCG-plasma reactions was measured using a spectral scanning multimode reader, and the final grouping results were automatically determined using a machine-learning strategy to avoid any subjective bias. A total of 3550 venous and finger-stick blood samples were tested on our paper-based assay to validate its accuracy. All human blood samples were primarily collected and tested for routine blood grouping or other clinical applications in Southwest Hospital (Chongqing, China). Blood groups were primarily identified by a diagnostic laboratory using the BioVue gel-card assay from Ortho Clinical Diagnostics Inc. Ten blood samples from uremic patients with an electrolyte disturbance were used to observe the effects of ionic strength on color definition and intensity.

Materials

NC membranes, filter paper, cotton linter paper, fiberglass, polyvinyl chloride (PVC) polymer, and the GF2 blood separation membranes were obtained from Jieyi Biotechnology. The blood separation membranes, including Vivid (GR), PES HD 1.8B, and MF1, were purchased from Pall, Cobetter, and Whatman, respectively. The blood preservation solution and blood collecting tubes containing either EDTA or sodium citrate were purchased from Weigao Biotechnology. The StabilGuard Immunoassay Stabilizer (protein free) was purchased from SurModics Inc. The heparin/lithium-treated blood-collecting tubes were from Sekisui Medical Technology. Polydimethylsiloxane (PDMS), BCG, polyoxyethylene alkyl phenol ether (Brij-35), citric acid, sodium hydroxide, dextran (average molecular weight, 35,000 to 45,000), NaOH, and NaCl were purchased from Aladdin Biotechnology. A series of micropipettes were purchased from Eppendorf, and ultrapure water (18.2 megohm) obtained from a Milli-Q Integral Millipore system was used throughout the study. Fluorescein isothiocyanate (FITC; F7250) was purchased from Sigma-Aldrich, and Cy3-labeled albumin was purchased from Sangon Biotech. Blood preservation solution was purchased from Nigale.

Anti-D, anti-C, anti-c, anti-E, and anti-e IgM antibodies against the antigens on the erythrocyte membrane were purchased from Alba Bioscience. Colorless anti-A IgM, anti-B IgM, standard A1 cells, and B cells were purchased from Libo Biotechnology Co. The antibodies against K and k were purchased from Merck Millipore, and the antibodies against M, N, S, s, P1, Jk^a, Jk^b, Le^a, Le^b, Fy^a, and Fy^b were purchased from Diagast (table S2).

This study was approved by the ethics committee of Southwest Hospital and performed in accordance with the Declaration of Helsinki and the *International Ethical Guidelines for Biomedical Research Involving Human Subjects*. Venous blood was stored in tubes with EDTA anticoagulant at 4°C after collection and before use, and finger-stick blood was used immediately. The blood group was identified by a diagnostic laboratory using the BioVue gel-card assay (Ortho Clinical Diagnostics Inc.) (*43*). Ten blood samples from uremic patients with an electrolyte disturbance were used to observe the effects of ionic strength on color definition and intensity (table S3). The absorbance of BCG-plasma reaction in different temperature, humidity, light intensities, and ionic strength was measured using Varioskan Flash (Thermo Fisher Scientific). Any detected weak D sample was further confirmed using a Coombs test, and the direct anti-human globulin reagents were purchased from Libo Biotechnology Co. A blood genotyping kit (BioSuper) based on polymerase chain reaction sequence-specific primers was used to recognize A_3.

Preparation of the BCG solution

After dissolving 0.105 g of BCG, 8.85 g of citric acid, 0.100 g of sodium azide, and 4 ml of Brij-35 (300 g/liter) in 950 ml of deionized water, the

solution was brought to pH 4.2 using a 6 M sodium hydroxide solution. Then, the volume was brought to 1 liter with deionized water. The final solution was stored at room temperature in a sealed polyethylene bottle for future use. The inclusion of a nonionic surfactant (Brij-35) reduces the absorbance of the blank, prevents turbidity, and provides linearity. Citric acid and sodium hydroxide were used to change the pH of plasma.

Preparation of the ABO forward format, ABD format, ABO F&R format, and ABO/Rh group assays

As illustrated in fig. S1A, each disposable paper-based strip consisted of a PVC substrate and a series of pads for sampling, RBC capture, and detection. A fiberglass mat was used as the sampling pad, and all other pads were fabricated with cotton linter paper. In a typical setting, the sampling pad was attached to the middle of the PVC strip, and two antibody pads were placed adjacent to the edges of the sampling pad, followed by the successive placement of a hydrophobic chromatography pad, a detection zone, and an absorbent pad on each side, with a 2-mm overlapping zone at each connection point. For ABO forward grouping, anti-A IgM and anti-B IgM were immobilized on opposite antibody pads, and BCG was immobilized on the two detection zones of the strip. ABD format assay was composed of quality control strip, A-test strip, B-test strip, and D-test strip (fig. S1B); the strip with no immobilized antibody (BCG only) was used for quality control strip to exclude nonspecific aggregation.

The antibodies were mixed with StabilGuard Immunoassay Stabilizer to retain the activities of antibodies after storage (*44*), and the impact of the storage time was investigated by storing the strips for 10, 20, 30, 60, 120, and 180 days. The antibody pad was immobilized with monoclonal IgM antibody by immersing the antibody pad in antibody solution for 10 min, followed by flow drying for 2 hours at 25°C (*45*). We introduced 10 μl of blood with the corresponding RBC antigens onto the strip and observed RBC agglutination after the strips were washed with PBS buffer to determine whether the antibodies were effectively immobilized (fig. S2D). In a typical experiment, the anti-A antibody (left) and anti-B antibody (right) were placed at different terminals to fabricate a disposable test strip for ABO blood grouping. Anti-D (left) and the blank were similarly used for Rh D grouping. The detection zone was prepared by soaking the substrate in the BCG solution for 10 min followed by drying in an oven (70° to 100°C) for 10 min or for 2 hours at 25°C. After assembly, the bulk substrate was cut into strips with dimensions of 50 mm × 2 mm × 0.6 mm. Then, sucrose was used to modify the strips, after which the individual strips were packed and stored at room temperature before use.

For simultaneous F&R ABO grouping, we designed two formats of strips (fig. S1B): the forward strip was identical to the strip described above, whereas the reverse strip used an additional blood separation pad to filter out any RBCs, mimicking the in vitro centrifugation procedure for plasma separation. For better plasma separation, a GF2 blood separation pad was used for sample loading instead of a fiberglass mat, and the other pads were composed of cotton linter paper. GF2 was dip-coated with blocking solution (0.5% sucrose) to increase the membrane hydrophilicity and the blood flow rate over the surface. After dip coating, the membranes were dried for 20 min at 50°C and then cut into 14-mm × 14-mm squares. In contrast to the forward strip, standard A1 or B cells were dropped onto the antibody pad to test the plasma antibody in the blood samples. Then, the two types of strips were pasted in parallel on one PVC substrate to consolidate the two sampling pads into one strip for the subsequent study. The positions of the anti-A/B IgM and the A/B erythrocytes were carefully controlled to facilitate the readout of the results in the combined assay. We immobilized anti-A on one side (left) and anti-B on the opposite side (right) of the forward strip, whereas type B RBCs were introduced on the left side and type A RBCs were introduced on the right side of the reverse strip, which was placed parallel to the forward strip.

As illustrated in Fig. 2C, our proposed ABO/Rh group assay was constructed on a transparent PDMS disc with several engraved microfluidic channels, and the centripetal ends were connected to a round sampling well that resembled a windmill. In a typical design, eight microfluidic channels were arrayed on the substrate with a ϕ = 3.2-mm sampling well, and each channel was embedded with a minimized strip (30 mm × 2 mm × 0.6 mm). The structure of the minimized strip was identical to the disposable POC strip, with only a single antibody (anti-A, anti-B, anti-C, anti-c, anti-D, anti-E, anti-e, anti-M, anti-N, anti-S, anti-s, anti-P1, anti-K, anti-k, anti-Jk^a, anti-Jk^b, anti-Le^a, anti-Le^b, anti-Fy^a, or anti-Fy^b) immobilized at the centripetal end of the strip. After the blood samples were pipetted into the sample well, the blood migrated within the strips via capillary action to react with specific antibodies. The eluent is the driving factor that induces a color change after the formation of the BCG-HSA/BCG–whole blood complexes.

Blood grouping

For fast blood grouping, 15 μl of fresh or anticoagulated whole blood was dropped onto the sample zone and incubated for 20 s to allow all specific RBCs to bind to the immobilized specific IgM antibody. Then, 30 μl of elution buffer was introduced to elute the nonagglutinated RBCs and plasma, followed by a color change in the detection zone within 30 s (fig. S16 and movie S1). For simultaneous F&R ABO group typing, 100 μl of whole blood was loaded on the sample zone, and 15 μl of whole blood was used for forward grouping, as described above. An additional 85 μl of blood was loaded onto the reverse strip and incubated for 1 min to allow complete plasma separation. Then, 10 μl of 20% diluted RBCs was applied to the antibody pad for 40 s and allowed to react with the agglutinins that may be present in the plasma. After the nonagglutinated erythrocytes and plasma were washed away with 60 μl of elution buffer, a color change was observed in the detection zone within 2 min.

For the F&R assay, if a type A blood sample (containing anti-B agglutinin in the plasma) is loaded, then a teal (left) and brown (right) color change will appear in both the forward and the reverse strips. In contrast, if a type B blood sample (containing anti-A agglutinin in the plasma) is loaded, then a brown (left) and teal (right) color change is observed in both channels. Note that the identification of type AB or O blood samples is relatively complicated because the loaded AB$^+$ blood will show two teal lines (F strip) and two brown lines (R strip), whereas type O blood will reveal two brown lines (F strip) and two teal lines (R strip).

For the ABO/Rh group assay, 80 μl of whole blood was loaded into the sampling well, followed by a 20-s incubation, and 120 μl of washing buffer was added to remove the unconjugated erythrocytes and plasma. The induced color changed was observed within 30 s, which can be read using a spectral scanning reader. Consequently the blood type results could be promptly given by using a machine-learning method (movie S2). An additional indirect Coombs' test was used to identify any weak D on paper strip. Briefly, the suspected Rh D samples were centrifuged (3000 rpm/min) for 1 min to remove any plasma. Then, the RBCs were rinsed three times using PBS buffer and incubated with IgG for 30 min at 37°C. After

washing away those unconjugated antibodies, the RBCs were resuspended to be 45% HCT, which could be loaded on the strip for the agglutination between these RBCs and the immobilized anti-human antibodies. All of the tests were conducted under natural light or a daylight lamp at room temperature and 40 to 70% humidity.

Methodology evaluation

Blood grouping is determined by a visual observation of the color changes (from yellow to teal/brown) in the detection zones. The teal color denotes that only plasma was detected (BCG-HSA), and brown indicates that whole blood was present (BCG–whole blood) in the detection zone. The reflectance value of the agglutinated or nonagglutinated RBCs in the detection zone was measured using a UV-3150 spectrophotometer (Shimadzu) to establish a quantitative readout of the blood types. The color intensity was obtained by subtracting the gray intensities of the red (R)/green (G)/blue (B) color channels using ImageJ 1.44p software (color intensity = 0.229R + 0.587G + 0.114B). A total of 3550 clinical blood samples were detected using the ABO forward, F&R, and multiple group assays, and the gel-card assay was adopted as a reference standard to verify the reliability of the proposed blood-grouping assay considering that the gel-card method is easy to handle and can obtain comparable results to the tube test (*46*). All figures were plotted using Origin Pro 8.6 software (OriginLab Corporation).

RBCs and HSA were fluorescently stained using previously described methods (*47*), with slight modifications, to improve the visualization of the RBC-antibody and BCG-HSA complexes. We modified the original staining strategy to obtain optimal results (fig. S17). Briefly, whole blood was centrifuged at 3000 rpm for 3 min to remove the plasma layer. The red cells were then washed with physiological saline (PSS) and incubated in a blood preservation solution with FITC (0.8 mg/ml) for 1 hour. The blood preservation solution was used to dissolve FITC. The blood preservation solution included 4.97 g of sodium chloride, 14.57 g of mannitol, 7.93 g of glucose, 0.14 g of adenine, 0.94 g of sodium dihydrogen phosphate, 1.5 g of sodium citrate, and 0.2 g of citric acid in each 1000 ml. The labeled RBCs were then washed with PSS and resuspended to achieve an HCT value of 45%. Eight microliters of the resuspended blood sample was pipetted onto the cotton linter paper on which the specific antibody was introduced to allow agglutinated blood clumps to form on the paper sheet. After a 20-s incubation, the linter paper was placed on a glass slide for fluorescence confocal imaging. Eight microliters of the Cy3-labeled HSA and FITC-labeled RBC mixture was dropped onto two strips (with or without antibody) to permit the clear observation of the nonagglutinated blood in the detection zone, and the detection zone was placed on a glass slide for imaging after elution. A Zeiss LSM 780 confocal microscope (Carl Zeiss SAS) was used to generate the confocal micrographs. The effects of temperatures and RHs on the BCG-HSA reaction have been tested using a temperature and humidity chamber H-150 (Spring Instrument Co.), and the effect of light intensities have been tested in artificial climate box PQX-250 (Spring Instrument Co.).

Machine-learning method for automated blood type identification

Because all the obtained data comprised a wavelength data set ranging from 200 to 1100 nm, we obtained 18 features by obtaining the mean values of these phases at 50-nm intervals. We considered the *F* scores when selecting the features for the feature vectors (*48*). Given training vectors x_k, where $k = 1, 2,\ldots, m$, if the number of positive and negative instances are n_+ and n_-, respectively, then the *F* score of the *i*th feature in the feature vector is defined as

$$F(i) = \frac{\left(\bar{x}_i^{(+)} - \bar{x}_i\right)^2 + \left(\bar{x}_i^{(-)} - \bar{x}_i\right)^2}{\frac{1}{n_+-1}\sum_{k=1}^{n_+}\left(x_{k,i}^{(+)} - \bar{x}_i^{(+)}\right)^2 + \frac{1}{n_--1}\sum_{k=1}^{n_-}\left(x_{k,i}^{(-)} - \bar{x}_i^{(-)}\right)^2}$$

where $\bar{x}_i, \bar{x}_i^{(+)}$, and $\bar{x}_i^{(-)}$ are the averages of the *i*th features of the whole, positive, and negative data sets, respectively; $x_{k,i}^{(+)}$ is the *i*th feature of the *k*th positive instance; and $x_{k,i}^{(-)}$ is the *i*th feature of the *k*th negative instance. Larger *F* scores correlate with more discriminative features.

LIBSVM (www.csie.ntu.edu.tw/~cjlin/libsvm/), a freely downloadable SVM package, was used to construct a classifier that was established in a CentOS5.4 system using LIBSVM3.12 and MATLAB R2013a. The data sets were divided into three dual-labeled groups: BCG–whole blood, BCG-HSA, and invalid tests. A radial basis function kernel was chosen as the more general form to improve the computational efficiency.

The classification algorithm was validated using 10-fold cross-validation tests. The original data set was randomly partitioned into 10 equal-sized subsets, where a single subset is retained as the validation data to test the model and the remaining subsets are used as the training data. Subsequently, the cross-validation process was repeated 10 times, in which each subset was used exactly once as the validation data set, and then all results from this process were averaged to produce a single estimate. The SVM parameter γ and penalty factor *C* were optimized in the 10-fold cross-validation tests using a grid search. The threshold for separating the positive and negative data sets was set to 0.5, which was the default setting in LIBSVM and was certainly optimal in the vast majority of tests when the data set was balanced. The performance of the prediction was assessed using four measures: accuracy, specificity, sensitivity, and the MCC, which were computed as follows

$$\text{accuracy} = \frac{\text{TP} + \text{TN}}{\text{TP} + \text{TN} + \text{FP} + \text{FN}}$$

$$\text{sensitivity} = \frac{\text{TP}}{\text{TP} + \text{FN}}$$

$$\text{specificity} = \frac{\text{TN}}{\text{TN} + \text{FP}}$$

$$\text{MCC} = \frac{\text{TP} \times \text{TN} - \text{FP} \times \text{FN}}{\sqrt{(\text{TP} + \text{FP})(\text{TP} + \text{FN})(\text{TN} + \text{FP})(\text{TN} + \text{FN})}}$$

Statistical analysis

Because the study was designed to develop a qualitative blood-grouping approach based on the combinational results of several reflective spectroscopic curves collected from distinctive observing window, most data were descriptive. A machine-learning strategy was used to automatically classify various blood types because any single point value cannot represent the trend of the comprehensive reflective spectroscopy curve. True positives (TP), false positives (FP), true negatives (TN), and false negatives (FN) are described in table S8. The MCC value is 1 for a perfect prediction and 0 for a completely random assignment. We performed statistics to compare the different intensities in absorbance of 630 nm or reflectance at 410 nm after different treatments. Data are expressed as

means ± SD from a minimum of four experiments, unless otherwise indicated. All statistical analysis was performed using SPSS 22.0 software package. For two-group comparisons, independent samples *t* test was used. For multiple-group comparisons, a one-way analysis of variance (ANOVA) with least significant difference post hoc test was used. $P < 0.05$ was considered to indicate a statistically significant difference. For experiments where $n < 20$, all individual-level data are shown in table S9.

SUPPLEMENTARY MATERIALS

www.sciencetranslationalmedicine.org/cgi/content/full/9/381/eaaf9209/DC1
Fig. S1. Schematics of the DAP assays.
Fig. S2. Improved performance of the DAP assay through optimized paper structure design and antibody immobilization.
Fig. S3. Optimized concentrations of reagents, RBCs, and antibodies.
Fig. S4. Stability of the immobilized antibodies and the optimal reaction time of the DAP assay.
Fig. S5. Stability of the BCG-plasma reaction according to pH and ionic strength.
Fig. S6. Results of samples with different HCT and HSA levels using the F&R assay.
Fig. S7. Influence of different blood storage times on the final results.
Fig. S8. Stability of the BCG-plasma reaction according to environmental factors.
Fig. S9. Relative reflectances of invalid samples.
Fig. S10. The receiver operating characteristic (ROC) curves and AUC of the samples.
Fig. S11. Images of the visual readout and reflectance spectra using the ABO forward and ABD assays.
Fig. S12. Images of the visual readout and reflectance spectra using the ABO F&R assay.
Fig. S13. Images of the visual readout and reflectance spectra using the ABO/Rh assay.
Fig. S14. Image of the visual readout and reflectance spectrum of a rare blood groups assay.
Fig. S15. The reproducibility of the DAP F&R assay.
Fig. S16. A brief instruction book for using the ABO forward strip.
Fig. S17. Confocal microscopic images of the FITC-RBCs prepared by using either the modified staining reagents or the traditional DMSO.
Table S1. Parameters of four types of plasma separation membranes.
Table S2. Monoclonal antibody details.
Table S3. Ionic strength change from blood samples of uremic patients.
Table S4. Accuracy of the ABO forward assay ($n = 800$) and ABD assay ($n = 50$).
Table S5. Accuracy of the ABO F&R assay.
Table S6. Accuracy of the ABO/Rh assay ($n = 1200$).
Table S7. Accuracy of other rare blood group assay ($n = 100$).
Table S8. Definitions of TP, FP, TN, and FN used in the machine-learning method.
Table S9. Individual level data for $N < 20$.
Movie S1. The testing procedure of fast ABO forward assay.
Movie S2. The testing procedure of ABO and Rh group multiplex antigen assay.

REFERENCES AND NOTES

1. J. T. Kirk, K. W. Lannert, D. M. Ratner, J. M. Johnsen, Serologic and phenotypic analysis of blood types via silicon nanophotonics. *Blood* **124**, 1565–1565 (2014).
2. L. T. Goodnough, J. H. Levy, M. F. Murphy, Concepts of blood transfusion in adults. *Lancet* **381**, 1845–1854 (2013).
3. L. T. Goodnough, Blood management: Transfusion medicine comes of age. *Lancet* **381**, 1791–1792 (2013).
4. H. G. Klein, I. Cortés-Puch, C. Natanson, Clinical practice: Blood-transfusion decisions not simple. *Nature* **521**, 289–289 (2015).
5. R. Ortega, R. J. Canelli, K. Quillen, W. Mustafa, F. Kotova, Transfusion of red cells. *N. Engl. J. Med.* **374**, e12 (2016).
6. A. Chung, P. Birch, K. Ilagan, A microplate system for ABO and Rh(D) blood grouping. *Transfusion* **33**, 384–388 (1993).
7. Y. Lapierre, D. Rigal, J. Adam, D. Josef, F. Meyer, S. Greber, C. Drot, The gel test: A new way to detect red cell antigen-antibody reactions. *Transfusion* **30**, 109–113 (1990).
8. D. M. Harmening, *Modern Blood Banking and Transfusion Practices* (FA Davis, 2012).
9. L. S. Chitty, M. Kroese, Realising the promise of non-invasive prenatal testing. *Brit. Med. J.* **350**, h1792 (2015).
10. C. Parolo, A. Merkoçi, Paper-based nanobiosensors for diagnostics. *Chem. Soc. Rev.* **42**, 450–457 (2013).
11. J. Hu, S. Wang, L. Wang, F. Li, B. Pingguan-Murphy, T. J. Lu, F. Xu, Advances in paper-based point-of-care diagnostics. *Biosens. Bioelectron.* **54**, 585–597 (2014).
12. W. Asghar, M. Yuksekkaya, H. Shafiee, M. Zhang, M. O. Ozen, F. Inci, M. Kocakulak, U. Demirci, Engineering long shelf life multi-layer biologically active surfaces on microfluidic devices for point of care applications. *Sci. Rep.* **6**, 21163 (2016).
13. T. Arbatan, L. Li, J. Tian, W. Shen, Liquid marbles as micro-bioreactors for rapid blood typing. *Adv. Healthc. Mater.* **1**, 80–83 (2012).
14. M. Li, J. Tian, M. Al-Tamimi, W. Shen, Paper-based blood typing device that reports patient's blood type "in writing". *Angew. Chem. Int. Ed. Engl.* **51**, 5497–5501 (2012).
15. M. S. Khan, G. Thouas, W. Shen, G. Whyte, G. Garnier, Paper diagnostic for instantaneous blood typing. *Anal. Chem.* **82**, 4158–4164 (2010).
16. D. R. Ballerini, X. Li, W. Shen, An inexpensive thread-based system for simple and rapid blood grouping. *Anal. Bioanal. Chem.* **399**, 1869–1875 (2011).
17. T. Songjaroen, W. Dungchai, O. Chailapakul, C. S. Henry, W. Laiwattanapaisal, Blood separation on microfluidic paper-based analytical devices. *Lab Chip* **12**, 3392–3398 (2012).
18. J. H. Spindler, H. Klüter, M. Kerowgan, A novel microplate agglutination method for blood grouping and reverse typing without the need for centrifugation. *Transfusion* **41**, 627–632 (2001).
19. M. Li, J. Tian, R. Cao, L. Guan, W. Shen, A low-cost forward and reverse blood typing device—A blood sample is all you need to perform an assay. *Anal. Methods* **7**, 1186–1193 (2015).
20. J. Granger, J. Siddiqui, S. Copeland, D. Remick, Albumin depletion of human plasma also removes low abundance proteins including the cytokines. *Proteomics* **5**, 4713–4718 (2005).
21. M. Ghaedi, H. Khajesharifi, A. H. Yadkuri, M. Roosta, R. Sahraei, A. Daneshfar, Cadmium hydroxide nanowire loaded on activated carbon as efficient adsorbent for removal of Bromocresol Green. *Spectrochim. Acta A Mol. Biomol. Spectrosc.* **86**, 62–68 (2012).
22. S. E. Smith, J. M. Williams, S. Ando, K. Koide, Time-insensitive fluorescent sensor for human serum albumin and its unusual red shift. *Anal. Chem.* **86**, 2332–2336 (2014).
23. J. Jopling, E. Henry, S. E. Wiedmeier, R. D. Christensen, Reference ranges for hematocrit and blood hemoglobin concentration during the neonatal period: Data from a multihospital health care system. *Pediatrics* **123**, e333–e337 (2009).
24. E. Anthes, Evidence-based medicine: Save blood, save lives. *Nature* **520**, 24–26 (2015).
25. S. G. Sandler, Blood group genotyping: Faster and more reliable identification of rare blood for transfusion. *Lancet Haematol.* **2**, e270–e271 (2015).
26. N. Houngkamhang, A. Vongsakulyanon, P. Peungthum, K. Sudprasert, P. Kitpoka, M. Kunakorn, B. Sutapun, R. Amarit, A. Somboonkaew, T. Srikhirin, ABO blood-typing using an antibody array technique based on surface plasmon resonance imaging. *Sensors* **13**, 11913–11922 (2013).
27. S. Paris, D. Rigal, V. Barlet, M. Verdier, N. Coudurier, P. Bailly, J.-C. Brès, Flexible automated platform for blood group genotyping on DNA microarrays. *J. Mol. Diagn.* **16**, 335–342 (2014).
28. W. Malomgré, B. Neumeister, Recent and future trends in blood group typing. *Anal. Bioanal. Chem.* **393**, 1443–1451 (2009).
29. M. C. Z. Novaretti, E. Jens, T. Pagliarini, S. L. Bonifácio, P. E. Dorlhiac-Llacer, D. A. F. Chamone, Comparison of conventional tube test with diamed gel microcolumn assay for anti-D titration. *Clin. Lab. Haematol.* **25**, 311–315 (2003).
30. W. L. Then, M. Li, H. McLiesh, W. Shen, G. Garnier, The detection of blood group phenotypes using paper diagnostics. *Vox Sang.* **108**, 186–196 (2015).
31. M. Li, W. L. Then, L. Li, W. Shen, Paper-based device for rapid typing of secondary human blood groups. *Anal. Bioanal.Chem.* **406**, 669–677 (2014).
32. A. Nilghaz, L. Zhang, M. Li, D. R. Ballerini, W. Shen, Understanding thread properties for red blood cell antigen assays: Weak ABO blood typing. *ACS Appl. Mater. Interfaces* **6**, 22209–22215 (2014).
33. A. K. Yetisen, M. S. Akram, C. R. Lowe, Paper-based microfluidic point-of-care diagnostic devices. *Lab Chip* **13**, 2210–2251 (2013).
34. S. Makulska, S. Jakiela, P. Garstecki, A micro-rheological method for determination of blood type. *Lab Chip* **13**, 2796–2801 (2013).
35. J.-Y. Chen, Y.-T. Huang, H.-H. Chou, C.-P. Wang, C.-F. Chen, Rapid and inexpensive blood typing on thermoplastic chips. *Lab Chip* **15**, 4533–4541 (2015).
36. D. D. Liana, B. Raguse, J. J. Gooding, E. Chow, Recent advances in paper-based sensors. *Sensors* **12**, 11505–11526 (2012).
37. W. L. Then, M.-I. Aguilar, G. Garnier, Quantitative blood group typing using surface plasmon resonance. *Biosens. Bioelectron.* **73**, 79–84 (2015).
38. J. Noiphung, K. Talalak, I. Hongwarittorrn, N. Pupinyo, P. Thirabowonkitphithan, W. Laiwattanapaisal, A novel paper-based assay for the simultaneous determination of Rh typing and forward and reverse ABO blood groups. *Biosens. Bioelectron.* **67**, 485–489 (2015).
39. S. Kawa, H. Oguchi, T. Kobayashi, M. Tokoo, S. Furuta, M. Kanai, T. Homma, Elevated serum levels of Dupan-2 in pancreatic cancer patients negative for Lewis blood group phenotype. *Br. J. Cancer* **64**, 899–902 (1991).
40. L. Hammar, S. Månsson, T. Rohr, M. A. Chester, V. Ginsburg, A. Lundblad, D. Zopf, Lewis phenotype of erythrocytes and Ie^b-active glycolipid in serum of pregnant women. *Vox Sang.* **40**, 27–33 (1981).

41. G. Daniels, *Human Blood Groups* (John Wiley & Sons, 2008).
42. L. Guan, J. Tian, R. Cao, M. Li, Z. Cai, W. Shen, Barcode-like paper sensor for smartphone diagnostics: An application of blood typing. *Anal. Chem.* **86**, 11362–11367 (2014).
43. R. Finck, C. Lui-Deguzman, S.-M. Teng, R. Davis, S. Yuan, Comparison of a gel microcolumn assay with the conventional tube test for red blood cell alloantibody titration. *Transfusion* **53**, 811–815 (2013).
44. N. Laboria, A. Fragoso, W. Kemmner, D. Latta, O. Nilsson, M. Luz Botero, K. Drese, C. K. O'Sullivan, Amperometric immunosensor for carcinoembryonic antigen in colon cancer samples based on monolayers of dendritic bipodal scaffolds. *Anal. Chem.* **82**, 1712–1719 (2010).
45. A. Apilux, Y. Ukita, M. Chikae, O. Chailapakul, Y. Takamura, Development of automated paper-based devices for sequential multistep sandwich enzyme-linked immunosorbent assays using inkjet printing. *Lab Chip* **13**, 126–135 (2013).
46. M. M. Langston, J. L. Procter, K. M. Cipolone, D. F. Stroncek, Evaluation of the gel system for ABO grouping and D typing. *Transfusion* **39**, 300–305 (1999).
47. L. Li, J. Tian, D. Ballerini, M. Li, W. Shen, A study of the transport and immobilisation mechanisms of human red blood cells in a paper-based blood typing device using confocal microscopy. *Analyst* **138**, 4933–4940 (2013).
48. Z. Ghahramani, Probabilistic machine learning and artificial intelligence. *Nature* **521**, 452–459 (2015).

Acknowledgments: We thank S. M. Zhao from the blood bank of the Southwest Hospital for critical review, Y. G. Liu from the Southwest University of Science and Technology for spectral analysis, Y. Z. Wu from the Third Military Medical University for statistical analysis, and Y. T. Fan for language proofreading. **Funding:** This work was supported by the National Natural Science Foundation of China (81572079 and 81371899), the Science Fund for Distinguished Young Scholars of Chongqing, China (CSTC2014JCYJJQ10007), the China Academy of Engineering Physics (WSS-2014-09), the Third Military Medical University (2015XZH11), and the Southwest Hospital (SWH2016ZDCX1017). **Author contributions:** Y.L. designed the study. H.Z. designed the mold of the strip and conducted antibody coating. H.Z. and X.Q. collected the spectral data. H.Z., X.Q., and L.Z. analyzed the data. Y. Yang, and Y. Zhu performed the confocal imaging. H.Z., X.Q., Y. Yang, Y. Zhou, and C.Q. generated the figures. X.Y. and K.Y. measured the color intensity. Y. Ye, Y. Zhou, and C.Q. carried out the gel-card blood grouping. Y.L., H.Z., X.Q., Y. Zou, X.Y., K.Y., Y. Ye, and Y. Zhou wrote and revised the manuscript. **Competing interests:** Y.L., H.Z., and X.Q. are inventors on patent applications (201510106835.X and 201510106833.0) submitted by Y.L. (Southwest Hospital, Third Military Medical University) that covers an ABO/Rh fast grouping method and an ABO F&R grouping method, respectively. **Data and materials availability:** All data in the paper are available from the corresponding author (luoyang@tmmu.edu.cn) upon request.

Submitted 20 April 2016
Accepted 24 February 2017
Published 15 March 2017
10.1126/scitranslmed.aaf9209

Citation: H. Zhang, X. Qiu, Y. Zou, Y. Ye, C. Qi, L. Zou, X. Yang, K. Yang, Y. Zhu, Y. Yang, Y. Zhou, Y. Luo, A dye-assisted paper-based point-of-care assay for fast and reliable blood grouping. *Sci. Transl. Med.* **9**, eaaf9209 (2017).

Science Translational Medicine
AAAS

A dye-assisted paper-based point-of-care assay for fast and reliable blood grouping

Hong Zhang, Xiaopei Qiu, Yurui Zou, Yanyao Ye, Chao Qi, Lingyun Zou, Xiang Yang, Ke Yang, Yuanfeng Zhu, Yongjun Yang, Yang Zhou and Yang Luo (March 15, 2017)
Science Translational Medicine **9** (381), . [doi: 10.1126/scitranslmed.aaf9209]

Editor's Summary

Finding the right type

Blood type matching is important for pregnancy, blood transfusion, and bone marrow transplantation. Zhang *et al.* developed a blood typing assay based on the color change that occurs when a common pH indicator dye reacts with blood. Red blood cells (RBCs) and plasma were separated from small volumes of whole, uncentrifuged blood samples using antibodies immobilized on paper test strips. The assays performed forward grouping (detecting A and/or B antigens on RBCs) and reverse grouping (monitoring the agglutination between RBCs and anti-A and/or anti-B antibodies in plasma) within 2 min and could also perform Rhesus and rare blood typing. A machine-learning algorithm grouped human blood samples automatically on the basis of spectral analysis of the colorimetric assay readouts. This economical and robust assay is useful for time- and resource-limited environments.

Science Translational Medicine (print ISSN 1946-6234; online ISSN 1946-6242) is published weekly, except the last week in December, by the American Association for the Advancement of Science, 1200 New York Avenue, NW, Washington, DC 20005.